Shock and Vibration 11 (2004) 47–66
IOS Press

Health monitoring of thick materials using piezoceramic patches, time signals, and wavelet transmittance functions

D.R. Hughes[a,*], A. Ghoshal[b], E. Rowe[a], M.J. Sundaresan[c], M.J. Schulz[d] and J.T. Feaster[a]
[a]*Naval Undersea Warfare Center, Division Newport, Newport, RI 02841-1708, USA*
[b]*NRC/Nondestructive Evaluation Sciences Branch, NASA Langley Research Center, Langley, VA 23681, USA*
[c]*Department of Mechanical Engineering, North Carolina A&T State University, Greensboro, NC 27411, USA*
[d]*Department of Mechanical Engineering, University of Cincinnati, Cincinnati, OH 45221-0072*

Received 6 April 2003
Accepted 5 August 2003

Abstract. A relatively overlooked factor in both global and local methods of health monitoring is the nonlinear stiffness of structures caused by the cycling of cracks and delaminations. Global methods of health monitoring use modal parameters or frequency response functions in an inverse procedure to quantify damage in structures with thick sections. Global approaches use fewer sensors that detect only significantly large damage in structures due to damage caused by transient vibration. However, local methods use Lamb wave propagation to detect small damage within a structure by an array of closely spaced sensors and actuators. Local methods also become more difficult to use on thick or non-homogeneous materials because wave propagation becomes complex. This paper develops a combined time series and wavelet analysis technique to improve damage detection in either thick, complex geometry, or non-homogeneous materials. A wavelet transmittance function (WTF) is defined as the ratio of continuous wavelet transforms from the time responses at different locations on a structure. A new damage indicator was developed based upon wavelet transmittance function. The novelty of the method lies in the fact that a near real time inference about the damage and the approximate extent of damage can be drawn without historical data. A simulated model is illustrated to highlight the potential of the new damage indicator on a thick aluminum specimen. Then, experimental signal data from two sets of different experiments conducted on thick structures with a crack and a delamination were analyzed using the wavelet transmittance function to detect the presence and extent of the damages as reflected on the WTF maps. This paper mainly deals with the development of WTF and the associated damage indicator by analyzing the simulated and experimental sets of data.

Keywords: Health monitoring, thick materials, piezoceramic sensors, wavelet transmittance function

1. Introduction

Many methods of damage detection are under investigation and these methods have been successful in laboratory settings using thin plate type structures. However, fewer investigations have considered damage detection in thick materials. Health monitoring becomes more difficult in thick materials, and non-homogeneous materials. It is considered here that strain vibration and strain wave propagation of structures contains information on the health of the structure and this information can be extracted by analyzing the time or time-frequency responses of the structure. As an example, cracks in vibrating structures, and particularly in thick structures, open and close (phenomena known as "crack breathing"), and this affects the amplitude of the time response [1–3]. These amplitude variations are difficult to detect and quantify using traditional Fourier analysis. Thus, time signal and time-frequency analyses are

*Corresponding author. E-mail: hughesdr@npt.nuwc.navy.mil.

ISSN 1070-9622/04/$17.00

investigated from which damage may be easier to detect and roughly quantify. Since much of vibration based damage detection theory is based on using the Fourier transform (FT), the limitation of the FT for analyzing transient signals is briefly discussed first. Then, a time signal and wavelet-based method of damage detection is proposed and experimentally investigated.

2. Damage detection theory

Modal analysis and frequency domain methods of damage detection are based on the Frequency Response Functions (FRFs) of a structure. Computationally, the FRFs are obtained by taking the Fourier Transform (FT) of the steady-state time responses, which is divided by the FT of the excitations of the structure. The FT is defined as:

$$f(\omega) = \int_{-\infty}^{\infty} f(t) e^{-j\omega t} dt \tag{1}$$

where $f(t)$ is the time function, $j = \sqrt{-1}$, t is time, and ω is radian frequency. The FT analyzes a signal using basis functions that extend for an infinite time. This is a good representation for steady-state stationary signals, however, transient signals within a steady-state signal are averaged out and their time reference is lost when the FT operation is performed. Thus, transient events from structures with damage may not be detected.

To overcome this limitation of the FT, the Short Time Fourier Transform (STFT) signal analysis method was developed in which a windowed function for the Fourier transform (FT) is used to examine a section of the time signal centered at a particular time u. The classical STFT defined by Gabor is:

$$\text{STFT} = f(u, v) = \int_{-\infty}^{\infty} f(t) g(t-u) e^{-ivt} dt, \tag{2}$$

where u is the translation of the window function and is the frequency [4]. Also, $f(t)$ is the given signal, and $g(t-u)$ is the window function. This transform is called the STFT because the multiplication by $g(t-u)$ localizes the Fourier integral in the neighborhood of $t = u$. By repeating the FT at each centered time window, this process will reveal if a particular frequency is present in the signal during that time segment. This linear time-frequency transformation localizes the signal content into frequency and time information. However, there is still a limitation of the STFT. The precision of the time and frequency information is determined by the size of the time window, which is constant for all frequencies when using the STFT. If the size of the time window could vary with frequency, this would increase accuracy. However, there is also a limitation here, the time and frequency resolution that can be obtained are dependent, and the time-frequency dependence is linked in the Heisenberg uncertainty principle [5]. Subject to the constraints defined by the uncertainty principle, wavelets can be developed to provide windowing with variable-sized regions. This produces more precise low and high frequency information.

3. Time-frequency resolution

The Heisenberg uncertainty principle states that the energy spread of a time function $f(t)$ and its Fourier transform $\hat{f}(\omega)$ cannot be simultaneously computed with arbitrarily small resolution. Gabor defined time-frequency atoms as waveforms that minimize the energy spread of a signal in the time-frequency plane. By windowing the area, the energy can spread for a particular Gabor atom in both time and frequency producing a Heisenberg rectangle. Ideally, this rectangle could shrink to a point that provides exact frequency information at any time. In actuality, the Heisenberg Uncertainty theorem shows that the minimum rectangular area achievable by a Gabor atom is:

$$\sigma_t \sigma_\omega \geqslant \frac{1}{2}, \tag{3}$$

where σ_t and σ_ω are the standard deviations that represent energy spread in the time and frequency domains, respectively. The definitions of the temporal variance and the frequency variance of the window function g are:

$$\sigma_t^2 = \frac{1}{\|g\|^2} \int_{-\infty}^{\infty} (t-u)^2 |g(t)|^2 dt \tag{4}$$

$$\sigma_\omega^2 = \frac{1}{2\pi \|g\|^2} \int_{-\infty}^{\infty} (\omega - v)^2 |\hat{g}(\omega)|^2 d\omega. \tag{5}$$

Furthermore, consider a scale factor applied to the Heisenberg Uncertainty principle. A scale applied to the definition of variance yields a Heisenberg rectangle with varying resolution. The scaled variance in time and frequency altered by the scale "a" yields:

$$\begin{aligned} \sigma_t^2 &= \int_{-\infty}^{\infty} \left(\frac{t-u}{a} \right)^2 |g_a(t)|^2 dt \\ a^2 \sigma_t^2 &= \int_{-\infty}^{\infty} (t-u)^2 |g_a(t)|^2 dt \\ \sigma &= a \sigma_{st} \end{aligned} \tag{6}$$

$$\sigma_\omega^2 = \frac{1}{a^2}\frac{1}{2\pi}\int_{-\infty}^{\infty}(a\omega - v)^2|\hat{g}_a(\omega)|^2 d\omega$$
$$\sigma_\omega^2 = \frac{1}{a^2}\sigma_{s\omega}^2. \tag{7}$$

This is the relationship between the scale parameter and the energy spread of the function in time and frequency as: $a\sigma_{st}$ and $\frac{\sigma_{s\omega}}{a}$, respectively [5]. This relationship explains how the wavelet transform can increase resolution in time thus emphasizing the frequency transients or non-linear characteristics in a signal. Smaller scales decrease the time spread and increase the frequency spread, which is shifted to higher frequencies while the area of the rectangles remains constant.

4. The continuous wavelet transform

A wavelet function $\psi(t)$ must satisfy certain criteria. Wavelets are functions in the Hilbert space (the Hilbert space is a vector space that has a norm, inner product, and Hermitian symmetry) and are written in the form; $\psi \in L^2(\Re)$, where $L^2(\Re)$ is the space of finite energy functions. These wavelets (ψ) have a zero average and their magnitude is bound through positive and negative infinite. The family of functions (ψ) whose axes shift in both time and scale are shown in the following generalized wavelet equation [6]:

$$\Psi_{a,u}(t) = \frac{1}{\sqrt{a}}\Psi\left(\frac{t-u}{a}\right). \tag{8}$$

The translation and scaling domains of the wavelet correspond to u and a in Eq. (8), respectively. Equation (8) also represents a normalized wavelet atom that is obtained by the translation and scaling of the mother wavelet ψ. The Continuous Wavelet Transform (CWT) is defined to be:

$$W_\psi(a,u) = \left\langle f(t), \Psi_{a,u}^*(t)\right\rangle = \int_{-\infty}^{\infty} f(t)\frac{1}{\sqrt{a}}\Psi^*\left(\frac{(t-u)}{a}\right)dt, \tag{9}$$

where Psi^* is the complex conjugate wavelet applied to the signal $f(t)$. Equation (9) produces CWT coefficients that are a function of scale and translation. With the complex form of Ψ, the separation of amplitude and phase components can be performed.

The Morlet wavelet is used as the CWT because it has a direct conversion between scale and frequency that is useful to show the frequency content of vibration signals. The Morlet wavelet used here is defined as [7]:

$$\Psi(t) = e^{i\omega_o|t|}e^{\frac{|t|^2}{2}}. \tag{10}$$

The $\Psi(t)$ wavelet is computed at the center frequency ω_o for every time point t. Thus, the Morlet wavelet has the advantage of computing the time-frequency plot for every frequency present within a signal. Also, the Morlet wavelet can be scaled to identify the effects of damage on the structural responses.

However, discrete wavelet analysis provides space-saving coding and is efficient for reconstruction. Although, continuous wavelet analysis is often easier to interpret since its redundancy tends to reinforce the traits. This is especially true for detecting subtle trends in sinusoidal like signals. Very few wavelets have an explicit analytical expression. Notable exceptions are the Mexican Hat and the Morlet wavelet. In contrast to the discrete wavelet transform, the CWT is also continuous in terms of shifting: during computation, the analyzing wavelet is shifted smoothly over the full domain of the analyzed function.

5. Transmittance functions

A Transmittance Function (TF) is the ratio of FRFs at two spatial locations on a structure. Transmittance functions can detect changes in the properties of a structure. The derivation of the TF is shown starting with the equations of motion for a structure:

$$M\ddot{x} + C\dot{x} + Kx = F(t) \tag{11}$$

where $x(t)$ is the displacement vector of a structure and M, C, K, are the mass, damping, and stiffness matrices, and $F(t)$ is the forcing vector. Performing the Laplace transform on Eq. (11) with zero initial conditions yields:

$$(Ms^2 + Cs + K)X(s) = F(s) \tag{12}$$

where $s = \sigma|j\omega$. Setting $\sigma = 0$ yields the Fourier transform, and rearranging gives:

$$X(j\omega) = H(j\omega)F(j\omega) \tag{13}$$

where $H(j\omega) = (-M\omega^2 + Cj\omega + K)^{-1}$ is the FRF matrix of the structure. Consider the case in which the excitation is applied at one point on the structure. Equation (13) becomes in matrix form:

$$\begin{bmatrix} X_1 \\ X_2 \\ X_3 \\ \vdots \\ X_n \end{bmatrix} = \begin{bmatrix} h_{11}\ h_{12}\ h_{13}\ldots h_{1n} \\ h_{21}\ h_{22}\ h_{23} \\ h_{313}\ h_{32} \\ \vdots \\ h_{nn} \end{bmatrix} \begin{bmatrix} 0 \\ F_2 \\ 0 \\ \vdots \\ 0 \end{bmatrix} \tag{14}$$

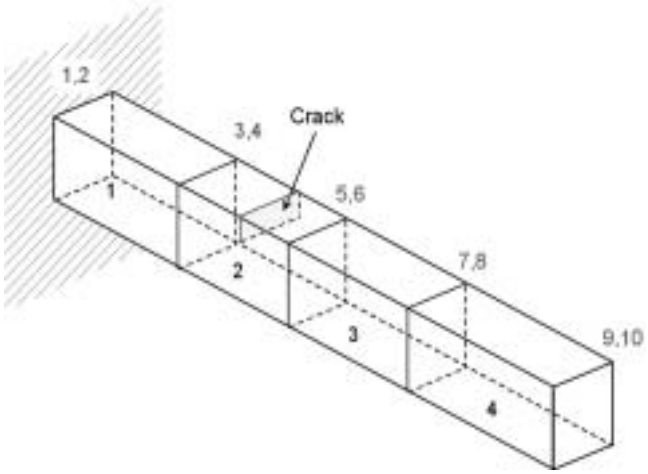

Fig. 1. Simulated Cantilever beam with Crack (a) Simulated Healthy Beam's 8-Element Model Time Signal. (b) Simulated Damage Beam's 8-Element Model Time Signal.

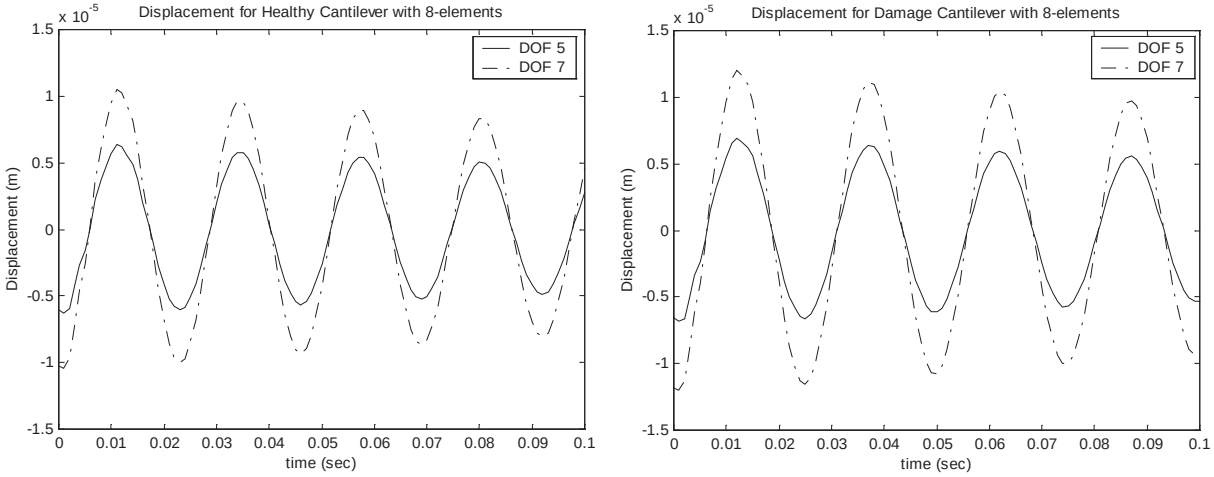

(a) Simulated Healthy Beam's 8-Element Model Time Signal.

(b) Simulated Damage Beam's 8-Element Model Time Signal.

Fig. 2. Simulated Time Signals from Transient Responses.

where only the force F_2 is nonzero. The TF between response points 1 and 2 on the structure is [8]:

$$T_{12} = \frac{X_1}{X_2} = \frac{h_{12}h_{22}^*}{h_{22}h_{22}^*} \tag{15}$$

The h_{12} and h_{22} are the individual FRFs for the response locations 1 and 2 on the structure due to a force at point 2 on the structure. For a single excitation, the TF is independent of $F(t)$. The complex TF quantifies the relative dynamic properties of a structure. As the response points 1 and 2 move spatially closer together, the TF approaches unity. Thus, the TFs of a structure can indicate levels of damage, which occur in the mass, damping, or stiffness parameters as a function of the frequency of excitation, and the effect of a single force is removed. The TF is very sensitive to damage because it is a ratio of functions with many peaks and valleys. The TF is based on the FT operation. As discussed, the FT has limitations in detecting nonlinear responses of structures due to damage. Therefore, the TF is extended to use wavelets.

Wavelet Transmittance Function (WTF) is developed as a quick signal processing method for damage detection. The WTF is written as [9]:

$$\text{WTF}_{1,2}(\omega, u) = \frac{W_\psi^1(\omega, u)}{W_\psi^2(\omega, u)}, \tag{16}$$

which is a real quantity in which the wavelet transform

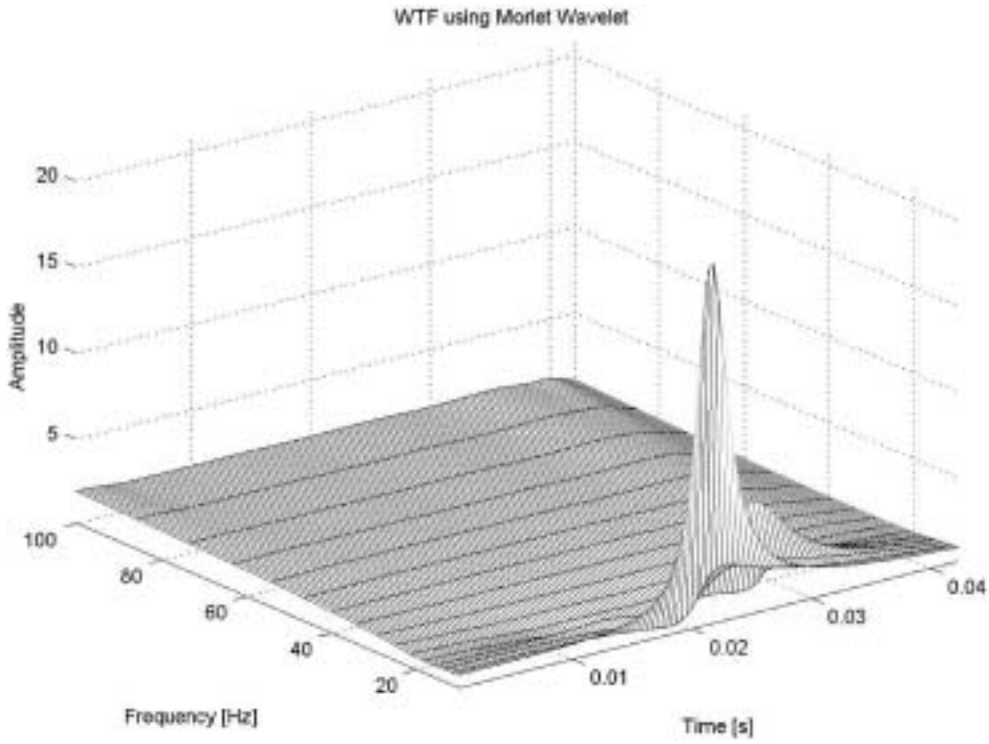

Fig. 3. WTF for both Simulated Healthy and Damage beam from Node 5.

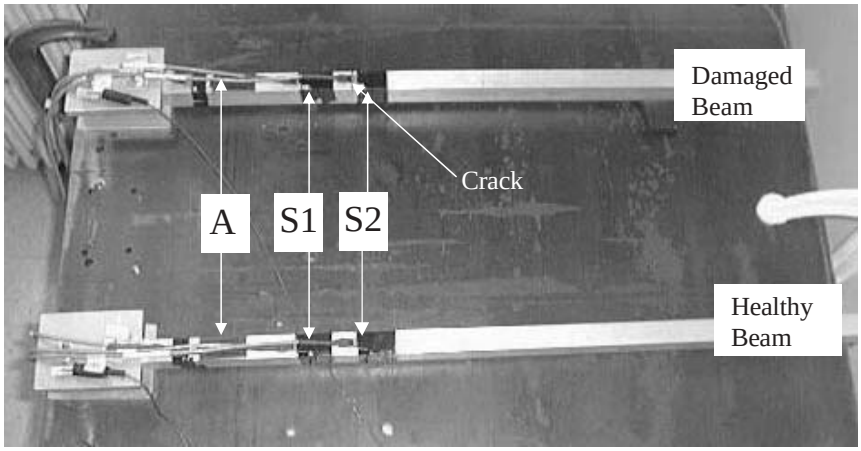

Fig. 4. Experimental setup.

$W_\psi^1(\omega, u)$ for sensor 1 is divided by $W_\psi^2(\omega, u)$ from sensor 2. The Morlet wavelet is used here in computing the WTF. Additionally, the mean amplitude S of the wavelet transform is:

$$S_{1,2} = \frac{1}{NPts} \sum_{n=1}^{Npts} \text{WTF}_{1,2}(n). \tag{17}$$

From this, a normalized damage indicator (NDI) is computed as:

$$\text{NDI}_{1,2} = \sum_{n=1}^{Npts} \frac{\left(S_{1,2}^h - S_{1,2}^d\right)^h}{S_{1,2}}. \tag{18}$$

Here S is the average of all the amplitude values in the WTF map, $Npts$ is the number of points in the 2-D wavelet map, h refers to the healthy structure, and d refers to the damaged structure.

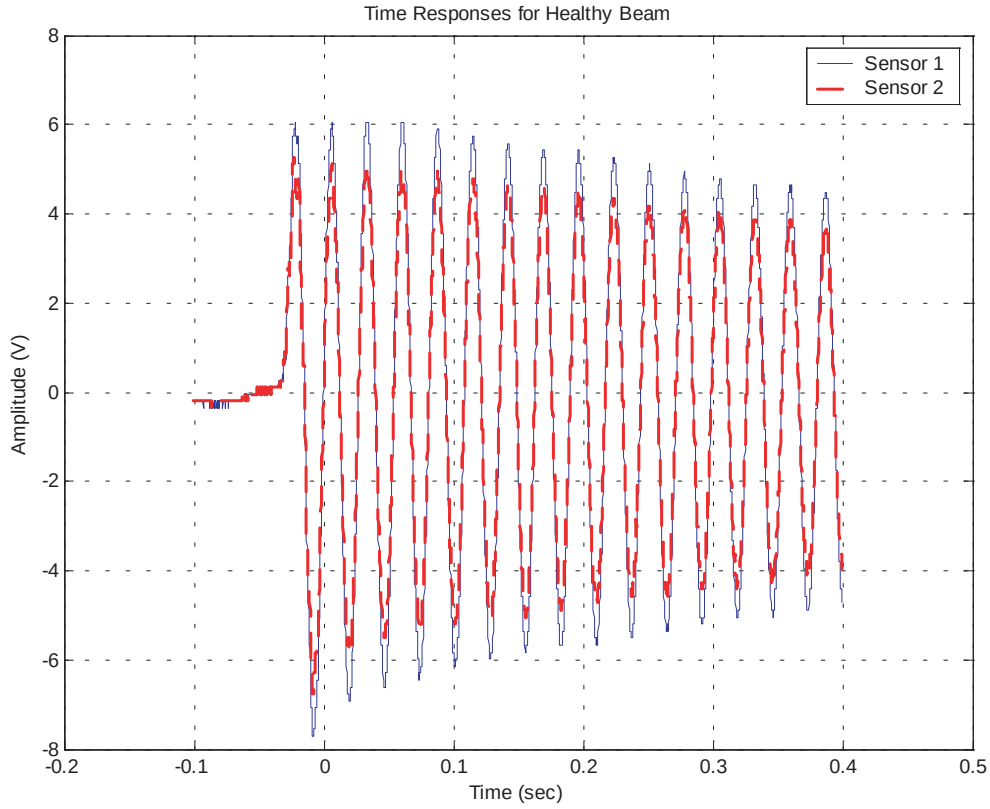

Fig. 5. Transient time responses for sensors S1 and S2 on the healthy beam. (a) Wavelet Transform from sensor 1 for the healthy beam. (b) Wavelet Transform from sensor 2 for the healthy beam.

6. Simulated damage detection in a thick aluminum beam using WTF and NDI

Damage detection in thick materials may need different approaches than the wave propagation methods used for thin plate structures [10–13]. To verify the potential of the WTF, a simple finite element Euler-Bernoulli beam model is developed. This analytical model is used to study the capability of WTF method to detect damage and to compare with the experimental results. However, this model is not a detailed fatigue crack finite element model, which simulates the high frequency acoustic emission generated from a crack closure. Instead, the model will provide a guide for interpreting the experiment. The model thus developed is sufficient to highlight the effectiveness of wavelet transmittance functions. In the simulated example, as described below, the WTF is applied to nodal vibration displacements of the damaged and healthy beams. The change in the displacement magnitude due to the presence of the crack would be reflected in the WTF map.

The simple finite element beam model consists of 8 beam elements. The simulated crack location is placed in the element where the actual physical crack is positioned on the beam described in detail in the next section of this paper. The dimensions of the simulated beam are $35 \times 1 \times 1.25$ inches in size. The simulated crack in the beam is 0.6 inch deep. The crack is 8.7 inches from the fixed-end of a cantilever beam. The simulation computes a damage case with the crack and a healthy case without the crack. Newton's Second Law of Motion is represented by the following equation:

$$M\ddot{y} + C\dot{y} + Ky = F(t), \tag{19}$$

where K is stiffness, M is mass, C is the damping, and F is the force applied to the system as a point load. Then, Newton's Second Law is converted into state-space form,

$$\begin{bmatrix} \dot{y} \\ \ddot{y} \end{bmatrix} = \begin{bmatrix} 0 & I \\ -M^{-1}K & -M^{-1}C \end{bmatrix} \begin{bmatrix} y \\ \dot{y} \end{bmatrix}, \tag{20}$$

to compute the set of linear equations and produces the displacement for the cantilever. Proportional damping

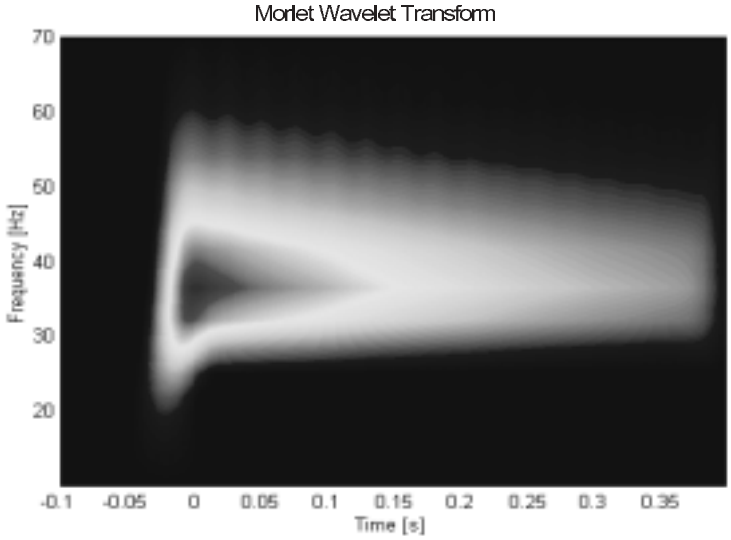

(a) Wavelet Transform from sensor 1 for the healthy beam.

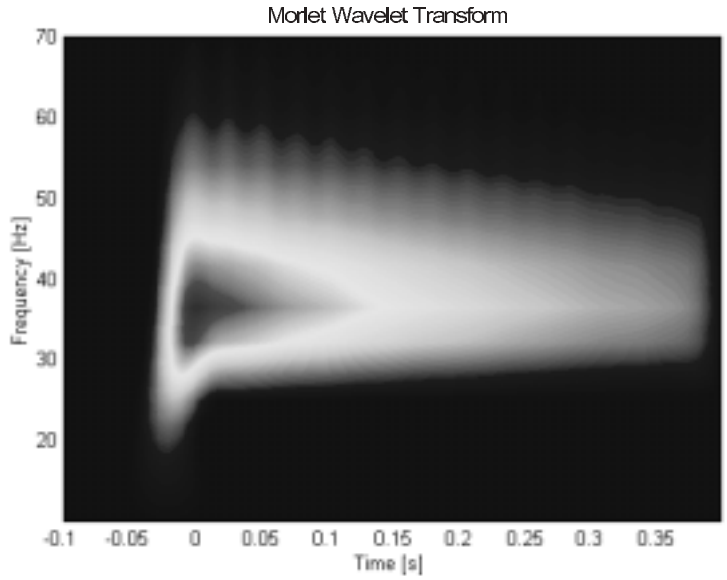

(b) Wavelet Transform from sensor 2 for the healthy beam.

Fig. 6. Wavelet Transform of the transient response of the healthy beam.

completes the matrices, and the initial displacement is given to y as a state-space vector. Figure 1 depicts a 4-element simulated cantilever that illustrates the positioning of the crack within the beam. The numbers separated by a comma on top of the beam represent the degrees-of-freedom (DOF), and the other numbers identify the element. With the state-space equations for an eight-element beam, Fig. 2(a,b) illustrates the displacement for DOF 5 and 7. The healthy beam has lower displacement amplitude in Fig. 2(a) at 43.1 Hz than the simulated damage beam in Fig. 2(b) at 38.1 Hz due to the stiffness reduction caused by the crack. Also, node 7 has higher displacement amplitude than node 5 for both cases, because cantilever deflection increases closer to the free-end of the beam. Figure 3 shows a WTF from the healthy and damage simulation at node 5 with S values of 0.9434 and 0.8366 from Eq. (17), respectively. The NDI from Eq. (18) is 0.1132, which confirms that stiffness changes within the beam are noticeable by this index.

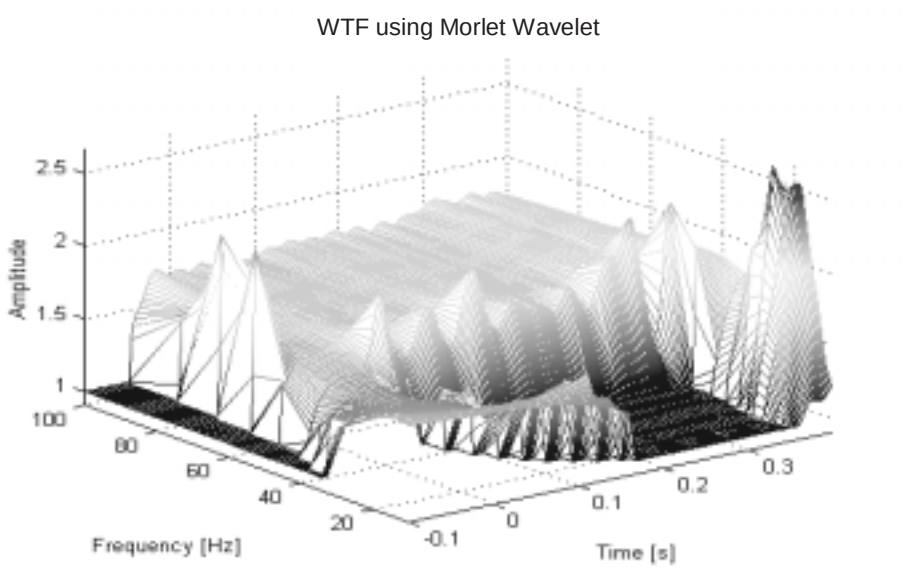

Fig. 7. WTF no clipping of the transient response of the healthy beam using sensors S1 and S2.

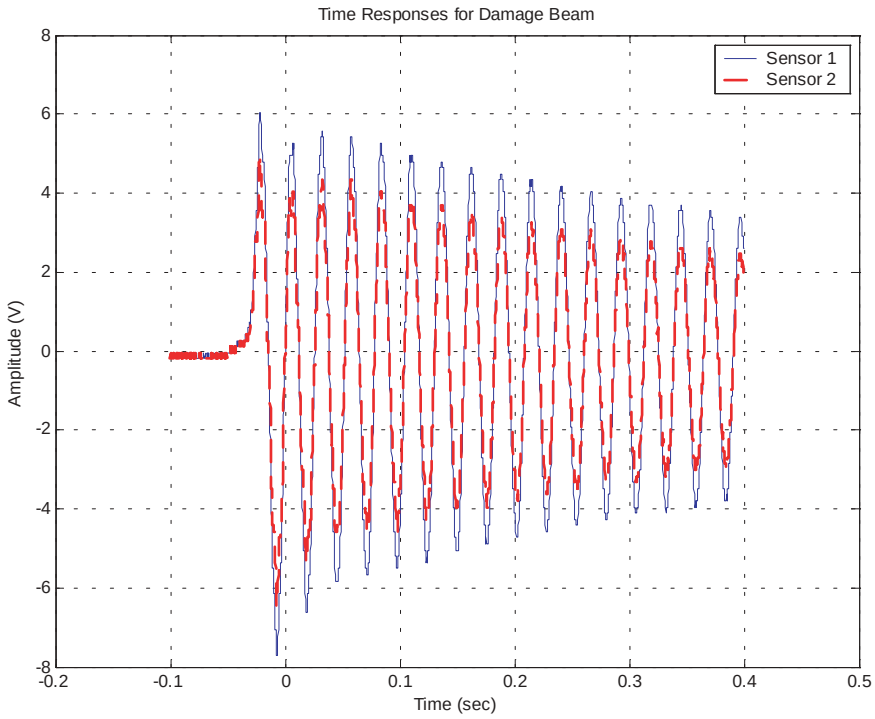

Fig. 8. Transient time responses for sensors S1 and S2 on the damage beam. (a) Wavelet Transform from sensor 1 for the damage beam. (b) Wavelet Transform from sensor 2 for the damage beam.

7. Experimentation

Experimental data from a thick aluminum beam with a fatigue crack and a thick composite flexbeam with an embedded delamination is analyzed using time signal analysis and wavelet analysis for detection of the damage and the extent of it. The experiments thus conducted and the analysis conducted thereof, are pre-

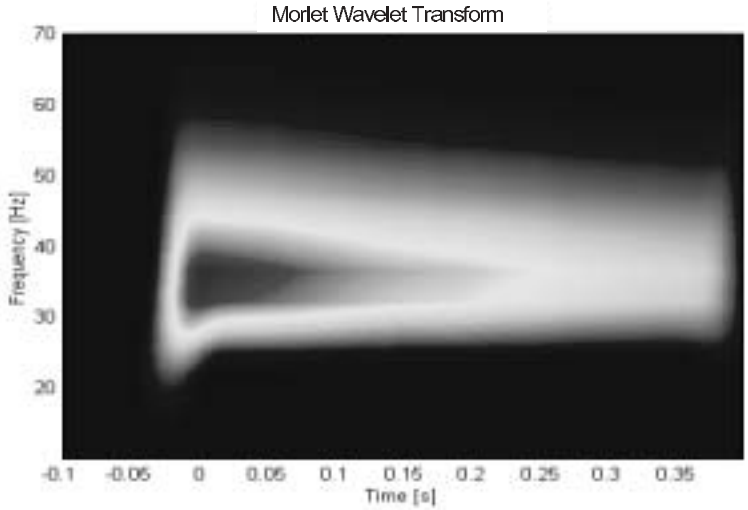

(a) Wavelet Transform from sensor 1 for the damage beam.

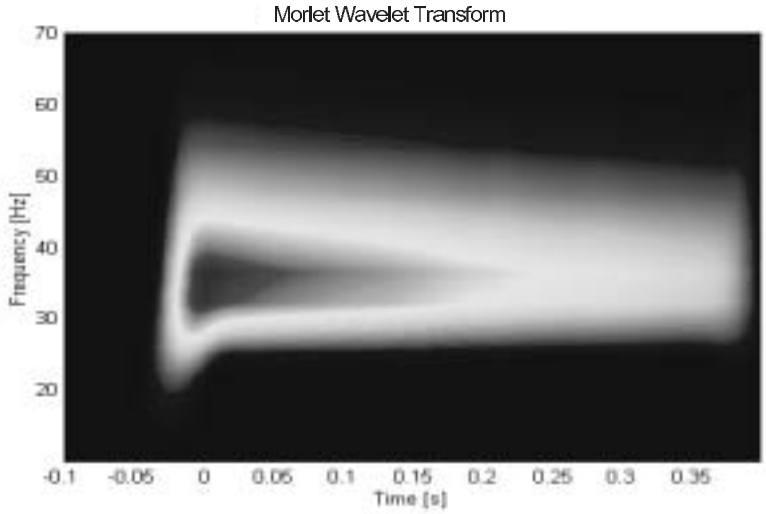

(b) Wavelet Transform from sensor 2 for the damage beam.

Fig. 9. Wavelet Transform of the transient response of the damage beam.

sented in the following sections.

8. Detection of a fatigue crack in a thick aluminum beam using WTF and NDI

One technique to identify changes or damage in structures is by analyzing the structural vibration [14–17]. Vibration signals measured before the onset of a crack will be different from the signals after a crack has formed. The fatigue crack will open and close causing frequency and amplitude changes in time waveforms. These frequency and amplitude variations are difficult to detect and quantify using Fourier analysis [18,19].

In this experiment, time waveforms captured from identical healthy and damaged beams are compared to determine the effect of a crack on the vibration response. The effectiveness of wavelet analysis to detect a fatigue crack in a beam is also investigated. Both beams as shown in Fig. 4 are $35 \times 1 \times 1.25$ inches in dimensions as noted in the above simulated example. The fatigue crack in the damaged beam is also indicated

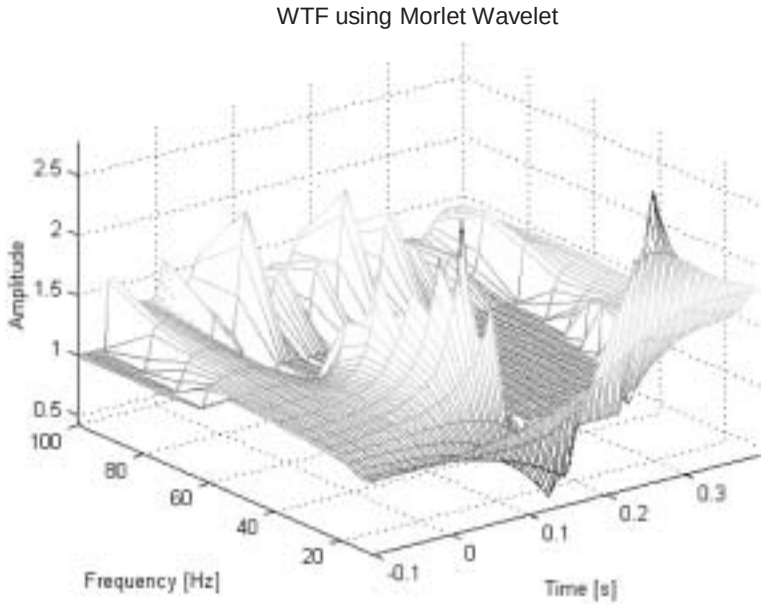

Fig. 10. WTF no clipping of the transient response of the damaged beam using sensors S1 and S2.

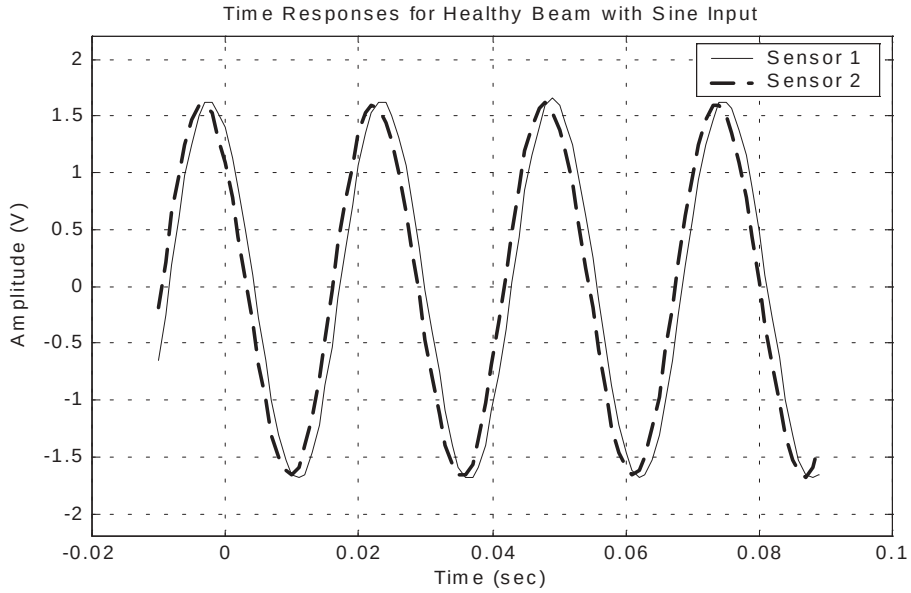

Fig. 11. Time responses of sensors S1 and S2 on the healthy beam for the sinusoidal input.

in Fig. 4. The size of the crack is 0.6 inch deep and the crack was grown from a 0.1 inch notch on the top of the beam. The fatigue crack was developed using a three-point-bend fixture, and the beam was cycled at its yield strength until the crack formed. The load was then reduced until the crack reached the desired depth. Figure 4 also shows two cantilever beams with three Lead Zirconate Titanate (PZT) patches attached to each beam. The PZT patch near the clamped end of the beam is used as the actuator (A). The second and third PZT patches are used as sensors (S1 and S2). The measurements were recorded by a LeCroy oscilloscope at a 10 kHz sampling rate and downloaded onto a PC hard drive through a RS-232 connection.

This objective of this experiment was to apply the WTF and NDI on the sensor outputs to identify a fa-

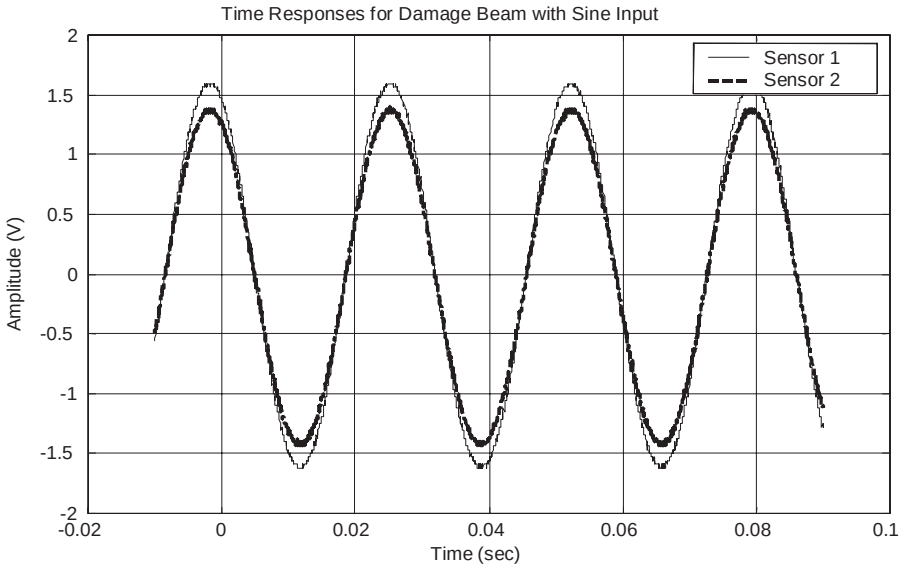

Fig. 12. Time responses of sensors S1 and S2 on the damage beam for the sinusoidal input.

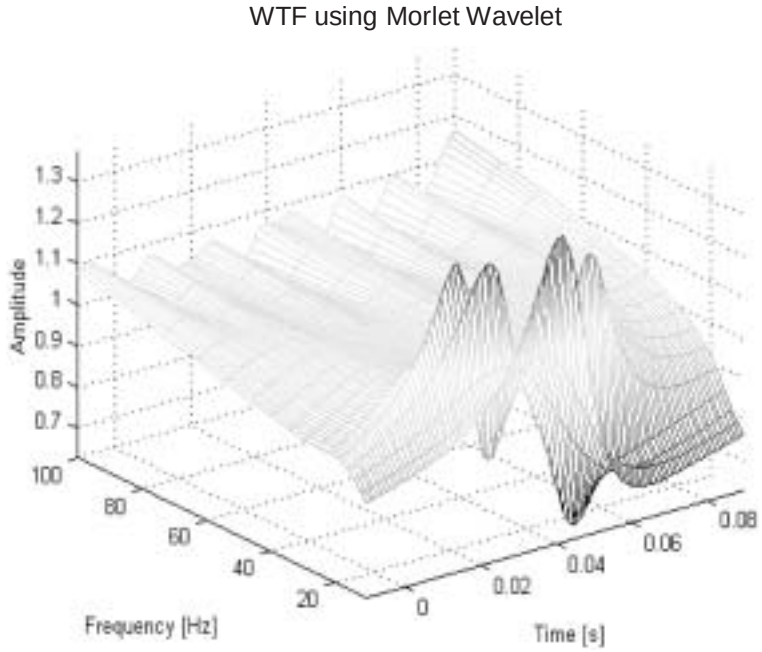

Fig. 13. WTF no clipping of the sinusoidal response of the healthy beam using sensors S1 and S2.

tigue crack in a cantilever beam. How the fatigue crack affects each beam can be determined by examining the strain vibration signals from sensors S1 and S2 for transient and sinusoidal excitations. Figure 5 shows the time responses from sensors S1 and S2 due to the free response of the healthy beam. The tip of the beam was initially displaced at the free end, for a known amount, to generate the free response. The first natural frequency of the healthy beam is found to be at 38.8 Hz. The time responses from sensors S1 and S2 as shown in Fig. 5 have a small amplitude difference that is associated with the location of the PZT sensors on the cantilever beam. The strain field is larger in S1 because of the larger bending moment closer to the fixed end

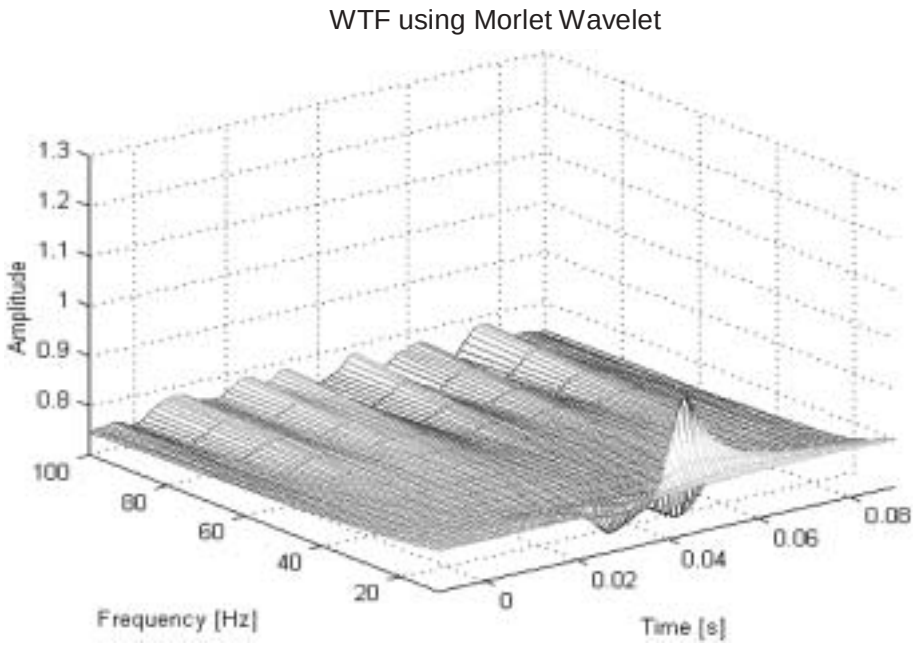

Fig. 14. WTF no clipping of the sinusoidal response of the damaged beam using sensors S1 and S2. (a) Helicopter rotor system (Picture Courtesy of Boeing Company). (b) Flexbeam tested.

of the beam. The wavelet transforms in Fig. 6 do not indicate any substantial differences in the responses of sensors S1 and S2 for the healthy case. The WTF for the free response of the healthy beam is computed using the signals from sensors S1 and S2 and is plotted in Fig. 7. The value from Eq. (23) is 1.6875 for the healthy beam. Figure 8 shows the time responses from sensors S1 and S2 due to the free response of the damaged beam. Figure 9 for the damage beam shows the wavelet transform plots for sensors S1 and S2. These wavelet transforms reveal the damage to the beam by the time required to reduce the amplitude of the time traces compared to Fig. 6. The WTF for the damaged beam is shown in Fig. 10. The S value is 1.2448 for the damaged beam, which has a natural frequency of 36.9 Hz. The free response of the damaged beam generates additional frequencies during the crack closure, which are apparent from the non-symmetric WTF map in Fig. 10. The NDI is 0.2623 for the transient input.

The steady-state sinusoid responses from the healthy beam are shown in Fig. 11. The steady-state sine responses from the damaged beam are shown in Fig. 12, which illustrates the stiffness reduction caused by the fatigue crack. This stiffness reduction creates an amplitude reduction in the WTF that is shown by comparing Figs 13 and 14. Corresponding to Fig. 13, the value is 1.0489 for the healthy beam. Corresponding to Fig. 14, the value is 0.7586 for the damaged beam with the sinusoidal input. The NDI is calculated as 0.2768. Thus, the NDI values confirmed there is damage present in the cracked cantilever beam using the transient and continuous excitations. Further testing would be necessary with different crack sizes to relate the damage size to the change in the WTF function. Note, that that while the transient response (sensor voltage) magnitude is four times larger than the sine response; the NDI values are almost the same for the two different excitation cases. This is because the WTF is a normalized damage indicator that removes the effect of the amplitude of the excitation.

Note that the wavelet plots have sporadic undulations that are caused by the WTF calculation. There can be computational error associated with division. Examples of this error are most clearly evident at 0.02 and 0.06 seconds in Fig. 13. The example numerically is the equivalent of dividing 0.0001 by 0.000001 that produces 100 as a WTF value. Thus, the frequency content is zero for the low frequency portion of the WTF plot. Also, there is a clipping algorithm to reduce the division error. Clipping creates the appearance of flat regions where the maximum amplitudes of two sensors are averaged and multiplied by a chosen percentage generating a cliplevel so the general trend of WTF plot is recognized. However, the clipping algorithm was not

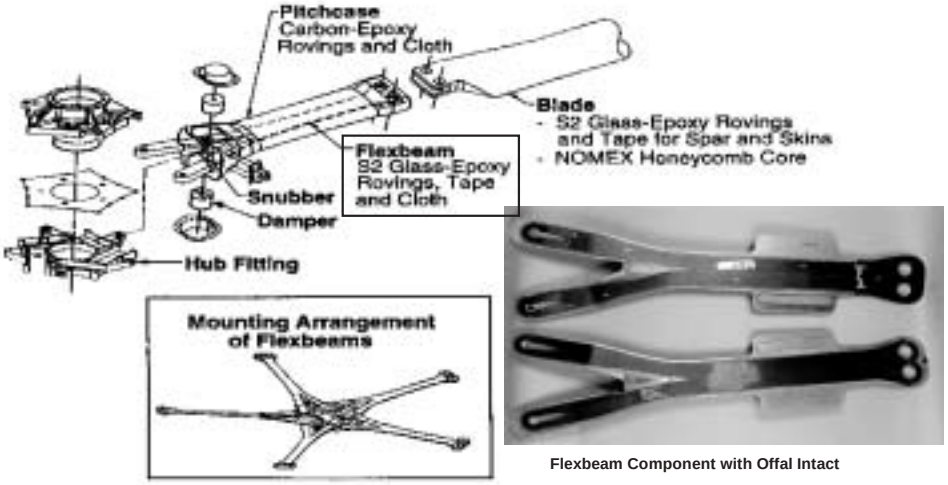

(a) Helicopter rotor system (Picture Courtesy of Boeing Company).

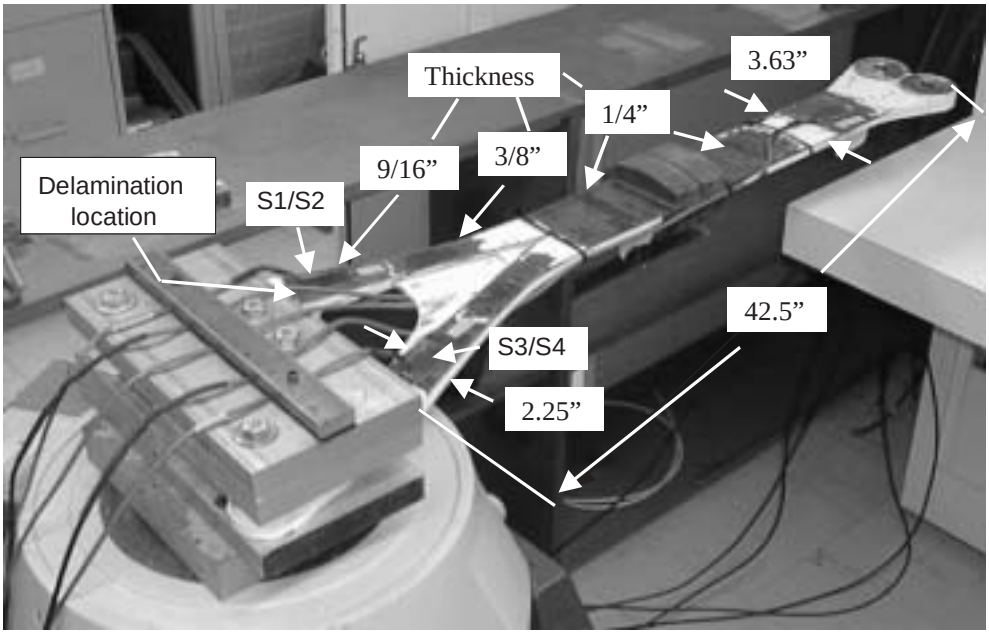

(b) Flexbeam tested.

Fig. 15. Schematic of a helicopter rotor system and a helicopter flexbeam.

used in all WTF plots, the flat regions often just appear planar however higher resolution reveals undulations.

9. Detecting delamination in a helicopter flexbeam

Detection of fatigue cracks and delaminations is an important area of current research in helicopter rotor systems. The rotor components shown in Figure 15 require high maintenance. If a health monitoring scheme for the rotor systems could be developed to continuously determine the structural integrity of these components, this would improve the safety and reliability of rotorcraft and significantly reduce maintenance costs. The function of the monitoring system is to detect any damage occurring to the flexbeam and rotor blade, to monitor the dynamic response of the rotor system for high levels, and to provide usage information on the health and the dynamic response of the rotor system.

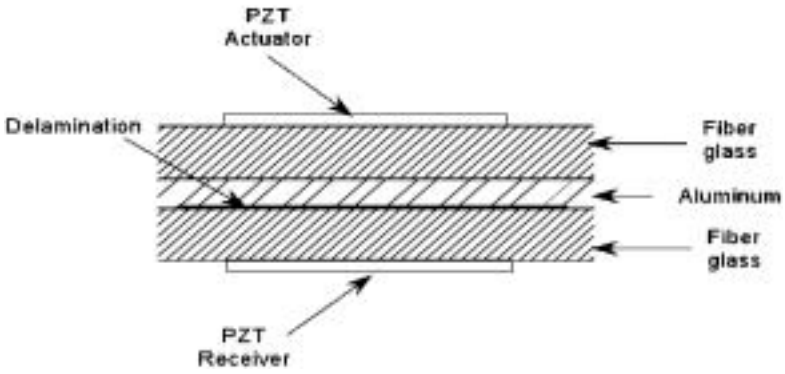

Fig. 16. Cross-section view of the flexbeam construction.

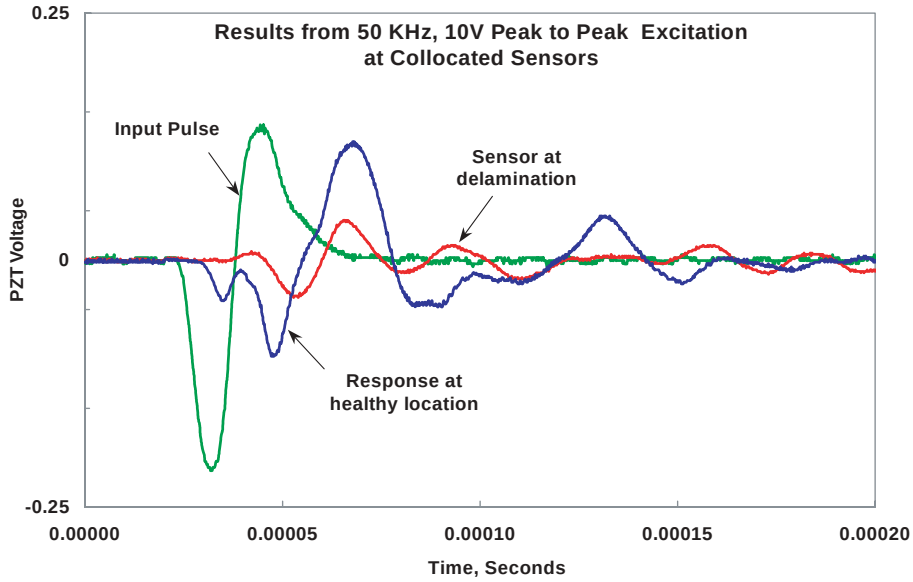

Fig. 17. Input, healthy, and damage time responses of the flexbeam for a 50 kHz sinusoidal burst excitation.

This information would be available immediately and can be used to define the performance limit for the helicopter based on the condition of the structure. The challenges in designing this monitoring system are related to the materials and operating conditions of the rotor system. The flexbeam where it attaches to the rotor is a critical section that is thick and non-homogeneous and is constructed using fiberglass with a center aluminum layer. The loading conditions include: significant aerodynamic and large dynamic loads, external damping in bending and torsion modes. Also, there is difficulty monitoring pure interrogation signals in the airborne (rotating blade) condition.

An experiment is performed using the flexbeam shown in Fig. 15(b). A single cycle sinusoidal burst of 50 kHz is simultaneously input through the PZT patches S1 and S3 in both the legs of the flexbeam and is sensed by the collocated sensors S2 and S4 underneath. The input from the signal amplifier is used as the trigger to acquire the signal by an oscilloscope. The actuators and sensors were also reversed to verify the reciprocity of the responses. Figure 16 shows the cross sectional arrangement of the collocated sensors and the actuators and the composite material constituting each of the legs of the flexbeam. Dimensions and the exact thickness were not given for proprietary reasons, but various thickness measurements are referenced in Fig. 15(b).

Figure 17 shows the input excitation and the output responses from the damaged leg sensor S2, and from the healthy leg sensor S4. Clearly there are three characteristics present in Fig. 17 that distinguish between

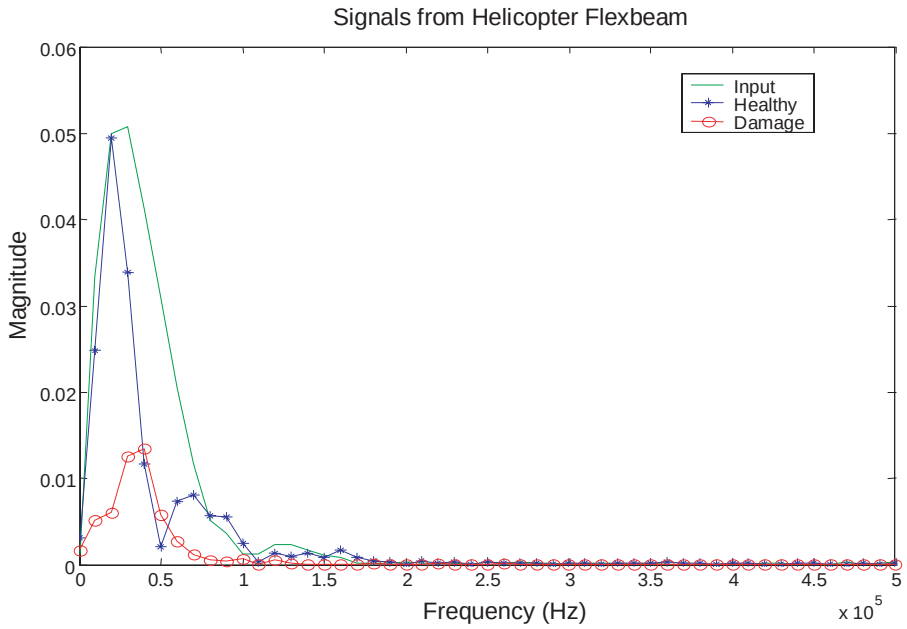

Fig. 18. FFT of the input, healthy, and damage responses of the flexbeam. (a) Contour plot of the 50 kHz sinusoidal input signal. (b) Mesh Plot of the 50 kHz sinusoidal input signal.

the healthy and the damaged leg responses. These are: (1) Time delay: The time delay between the input excitation and the response of sensor S4 in the healthy leg is distinctly shorter than the response of sensor S2 in the damaged leg; (2) Waveform characteristics: The waveform patterns from the sensors in the two legs have significantly different shapes; and (3) Leading Edge amplitude: The leading edge amplitude of the output waveform obtained from the sensor S2 in the damaged leg is clearly attenuated compared to the leading edge amplitude of the output waveform obtained from the sensor S4 in the healthy leg. To explain this behavior, referring to Fig. 16, the high frequency moment actuated on the top of the leg is not fully transferred to the bottom of the leg due to the delamination. Thus, the bottom patch on the leg with the delamination has a reduced and delayed strain response. An optimal excitation frequency in the range of 50 kHz to 75 kHz was chosen to locate damage and provide sufficiently large signal amplitude considering the excitation frequency, wavelength, and size of the PZT patch. Figure 18 is a FT of the signals and shows that the maximum energy occurs near 35 kHz for the input signal, 20 kHz for the healthy signal, and 35 kHz for the damaged signal. When exciting at low frequencies below 1 kHz, the global vibration modes of the flexbeam are excited and the damage is not obvious.

The wavelet transforms of the time responses are shown in Fig. 19 using the Morlet wavelet. Figures 19(a, b) give the contour and mesh wavelet plots for the input excitation, respectively. Figures 19(a, b) show that the amplitude is large for the frequency range for the input excitation from 0 to 60 kHz with maximum energy intensity near 35 kHz, occurring from 0.5ms to 0.75ms. The output response in Figs 20(a, b) from the healthy leg sensor S4 is given in the contour and mesh wavelet plots. The frequency range shown in Figs 20(a, b) of the healthy leg response at S4 is between 0 and 30 kHz with the maximum energy intensity occurring around 20 kHz from 0.25ms to 1.2ms. Figures 21(a, b) show the contour and mesh wavelet plots for the output response from the damaged leg sensor S2 near the delamination. The Figs 21(a, b) also show that the frequency range for the damaged leg output response at S2 is between 10 kHz and 50 kHz with maximum energy intensity at around from 0.4ms to 0.1ms.

Clearly the time delay in the output response from the damaged leg sensor S2 near the delamination is longer than the output response from the healthy leg sensor S4. Also, the amplitude of the maximum energy for the healthy response ($\sim$2.5) is larger than for the damaged response ($\sim$0.25). This may occur because the material in the flexbeam attenuates the responses and the higher frequencies are suppressed as shown by comparing the input excitation with the output response from the healthy leg sensor in Figs 19 and 20. However, the higher frequencies are reintroduced in the response

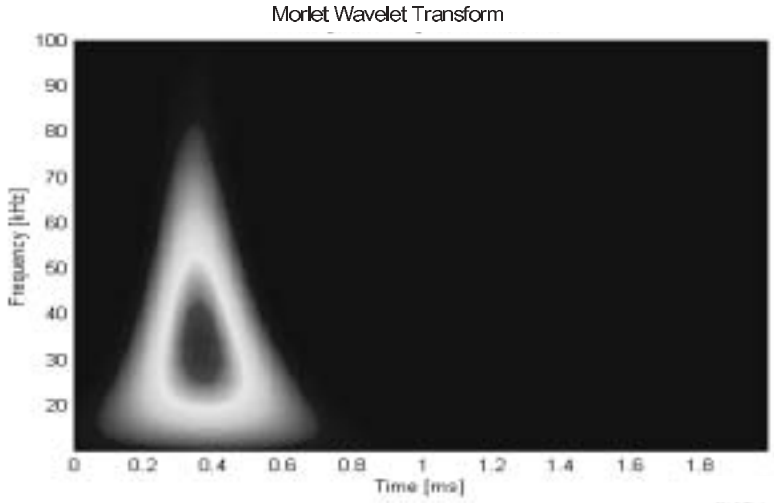

(a) Contour plot of the 50 kHz sinusoidal input signal.

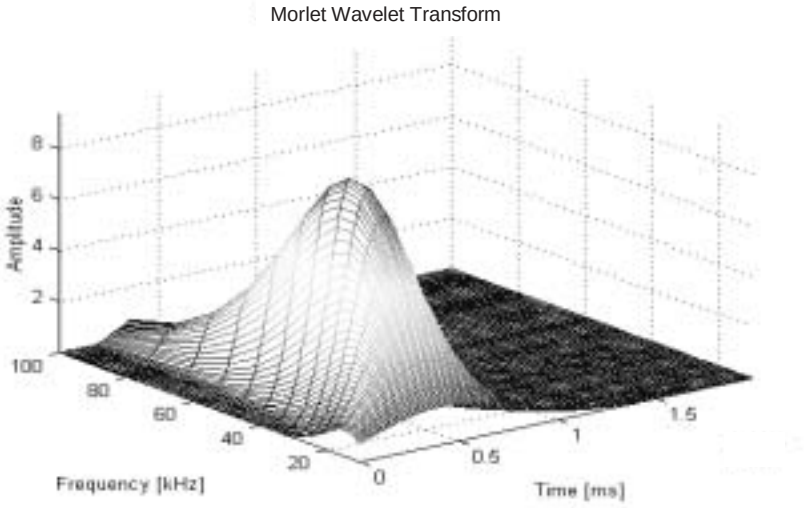

(b) Mesh Plot of the 50 kHz sinusoidal input signal.

Fig. 19. Wavelet plots of the 50 kHz sinusoidal input signal. (a) Contour plot of the healthy response from sensor S4. (b) Mesh plot of the healthy response from sensor S4.

from the damaged leg as shown in Fig. 21 Energy during the "crack breathing" from the delamination may be converted into higher frequencies in the time waveform causing higher frequency scattering in the wavelet map.

Additionally, the WTF was investigated to determine how well this technique would quantify the non-linear effects created by the damage. The WTF was computed from the healthy and damaged leg of the flexbeam as shown in Fig. 22(a,b). At one percent clipping the pattern became apparent in Fig. 22(a,b) with some spurious peaks, however, the pattern at five percent clipping is clear in Fig. 22(a,b). This outline may represent the frequency-time region in which structural health monitoring could be conducted. A structural health monitoring technique could use the time axis to identify when the delamination readmits the high frequency components into the signal, and thus the location of damage through the depth of the flexbeam might be calculated. Dominant energy levels are depicted by the frequencies present in the time waveforms. This frequency content information could be utilized in a control algorithm to maintain structural integrity for in-flight reliability. Monitoring complex systems like the helicopter rotor system using WTFs can improve safety

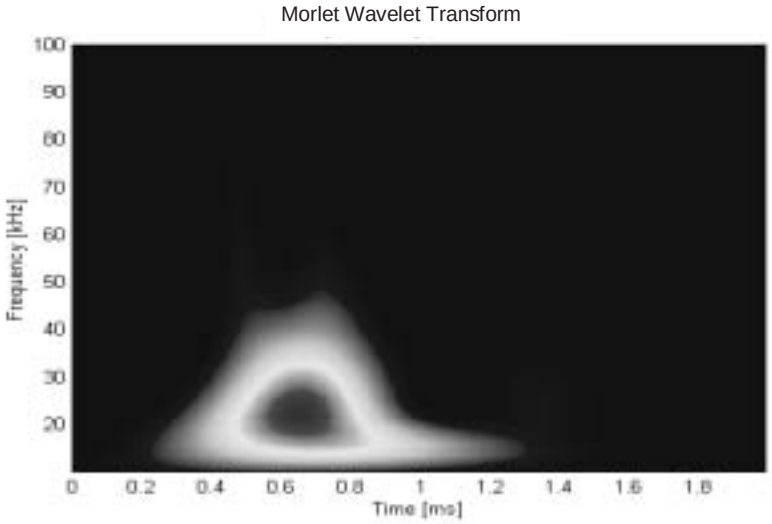

(a) Contour plot of the healthy response from sensor S4.

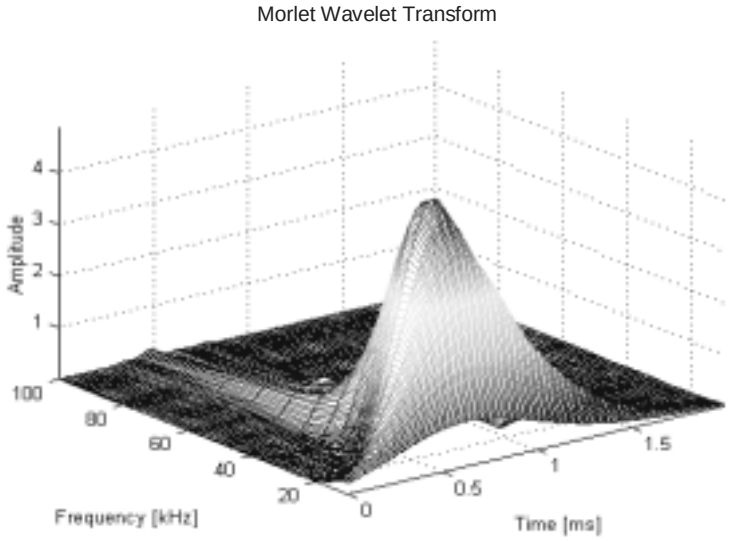

(b) Mesh plot of the healthy response from sensor S4.

Fig. 20. Wavelet plots of the response of the healthy leg of the flexbeam. (a) Contour plot of the damage response from sensor S2. (b) Mesh plot of the damaged response from sensor S2.

and reduce maintenance cost. However, environmental effects such as variations in flight speed could create additional non-linear behavior that has not been taken into account in this research. Note the WTF's amplitude is normalized to eliminate some environmental effects, which would prove beneficial on an actual rotor system. Further research is required to fully determine the sensitivity of the WTF method. This research should include vibrating the flexbeam transversely and using the four patches as sensors only to measure the strain responses and compute WTF's to detect damage. This would be a passive technique to detect damage and would simplify health monitoring on an operating helicopter.

10. Conclusions

When a fatigue crack or delamination opens and closes the stiffness of the structure changes and this

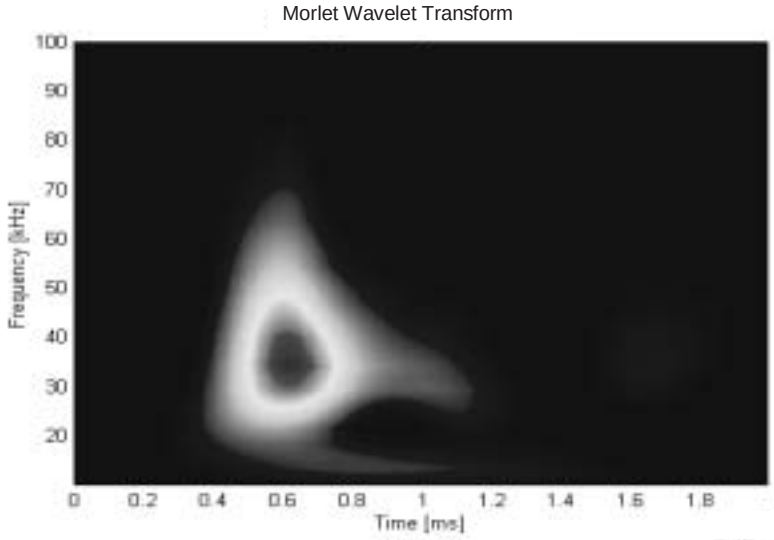

(a) Contour plot of the damage response from sensor S2.

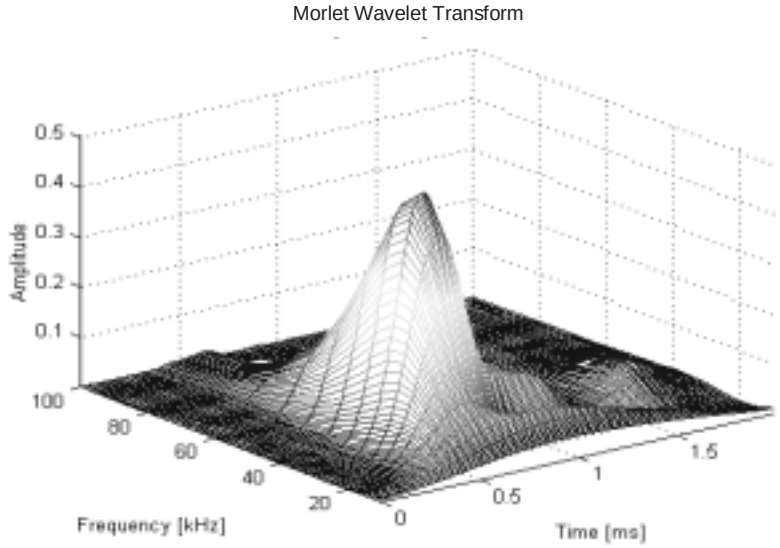

(b) Mesh plot of the damaged response from sensor S2.

Fig. 21. Wavelet plots of the response of the damage leg of the flexbeam at sensor S2. (a) WTF 5% clipping contour plot using the damaged (sensor S2) and healthy responses (sensor S4) (a) WTF 5% clipping mesh plot using the damaged (sensor S2) and healthy responses (sensor S4).

causes frequency and time variations in the vibration response of the structure. These frequency and time variations are difficult to detect and quantify using conventional signal processing techniques. Accordingly, time-frequency analyses and dynamic strain signals were investigated to provide a more positive indication of damage. The simulated and the experimental data verified the effectiveness of using PZT patches bonded on the surfaces of thick aluminum and non-homogeneous composite materials for sensing known variations in time waveforms due to a fatigue crack or delamination. Furthermore, this approach is a simpler and less expensive method than embedding sensors in a material, which cannot be done in many applications.

This research highlights the potential of wavelet analysis to identify a fatigue crack using wavelet transforms due to their filtering capabilities. Thus, the wavelet transform has the potential to identify certain frequency content within broadband noise. Therefore, crack closures create high frequency acoustic waves

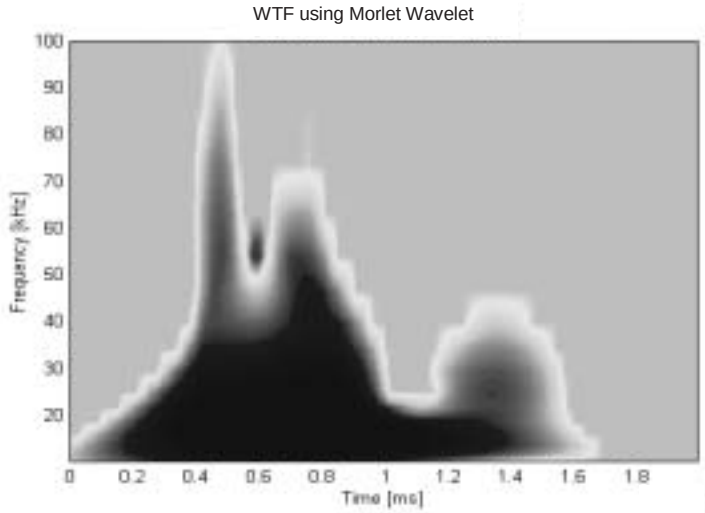

(a) WTF 5% clipping contour plot using the damaged (sensor S2) and healthy responses (sensor S4)

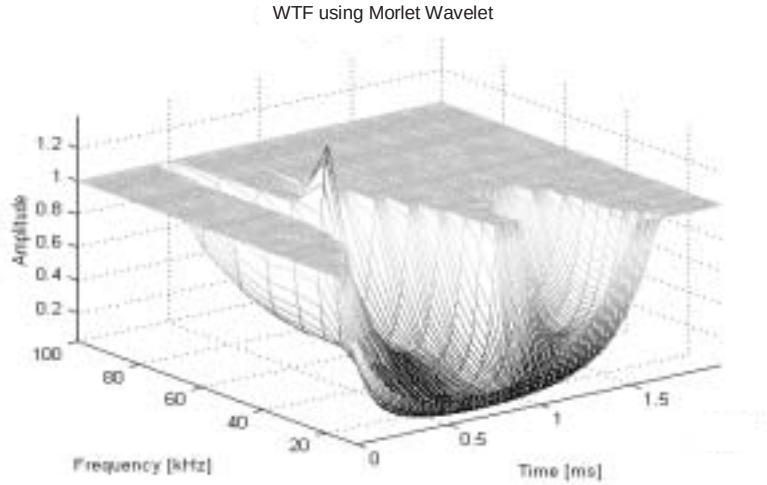

(a) WTF 5% clipping mesh plot using the damaged (sensor S2) and healthy responses (sensor S4)

Fig. 22. WTF plots for the damaged helicopter flexbeam.

and the ambient noise creates broadband noise. The wavelet signal processing technique has the ability to isolate the dominant energies or frequencies present within those time signals. However, a pure transmittance function does not filter data; and, as a result, transmittance is often very difficult to interpret. By filtering the noise out of the time signal in the wavelet transform the resulting WTF produces a NDI, which is a meaningful value that can evaluate structural integrity. An application of the wavelet transform and WTF also produced meaningful results concerning the amplitude and time variations that happen due to delaminations in a helicopter flexbeam. Also, the WTF's amplitudes normalize the energy levels present in the time waveforms minimizing the environmental effects, which make the technique suitable for practical use. Most importantly, a region was shown that may identify the time and frequency information useful for damage quantification.

Acknowledgement

This work was supported by the NASA Center for Aerospace Research at North Carolina A&T State University, the NASA Ronald E. McNair Fellowship, and

the NASA Rotorcraft Center of Excellence at Penn State University. The students and faculty appreciate this support.

References

[1] M.H.H. Shen and Y.C. Chu, Vibrations of Beams with a Fatigue Crack, *Computers and Structures* **45**(1) (1992), 79–93.

[2] B.P. Nandwana and S.K. Maiti, Modeling of Vibration of Beam in Presence of Inclined Edge or Internal Crack for Its Possible Detection Based on Frequency Measurements, *Engineering Fracture Mechanics* **58**(3) (1997), 193–205.

[3] B.P. Nandwana and S.K. Maiti, Detection of the Location and Size of a Crack in Stepped Cantilever Beams Based on Measurements of Natural Frequencies, *Journal of Sound and Vibration* **203**(3) (1997), 435–446.

[4] P.M. Bentley and J.T.E. McDonnell, Wavelet Transforms: An Introduction, *Electronics & Communication Engineering Journal* (August 1994), 175–186.

[5] S.G. Mallat, A Wavelet Tour of Signal Processing 2nd Ed. New York: Academic Press, 1999.

[6] S. Hahn, *Hilbert Transforms in Signal Processing*, Artech House, Inc, 1996.

[7] P.M. Bentley and J.T.E. McDonnell, Wavelet Transforms: An Introduction, *Electronics & Communication Engineering Journal* (1994), 175-186.

[8] H. Zhang, M.J. Schulz, A.S. Naser, F. Ferguson and P.F. Pai, Structural Health Monitoring using Transmittance Functions, *Mechanical Systems and Signal Processing* **13**(5) (1999), 765–787.

[9] D.R. Hughes, *Damage Detection using Wavelet Analysis*, Ph.D. thesis, North Carolina A&T State University, 2001.

[10] J. Qu, Interface Crack Loaded By a Time-Harmonic Plane Wave, *International Journal of Solids Structures* **31**(3) (1994), 329–345.

[11] J. Qu, Reflection of Elastic Waves By a Randomly Cracked Interface, Ultrasonic Characterization and Mechanics of Interfaces, *AMD-Vol* **177** (1993), ASME.

[12] J. Qu, Scattering of Plane Waves from an Interface, *International Journal of Engineering Science* **33**(2) (1995), 179–194.

[13] D.J. Pines, *The Use of Wave Propagation Models for Structural Damage Identification*, Proceedings of the International Workshop on Structural Health Monitoring, Stanford, CA, 1997, 665–677.

[14] W.J. Staszewski, Structural And Mechanical Damage Detection Using Wavelets, *The Shock and Vibration Digest* **30**(6) (1998), 457–472.

[15] Y.Y. Kim and E.H. Kim, *New Damage Detection Method based on Wavelet Transform*, IMAC-XVIII, II, 2000, 1207–1212.

[16] C.J. Lu and Y.T. Hsu, *Application of Wavelet Transform to Structural Damage Detection*, IMAC-XVII, I, 1999, 908–914.

[17] G. Catalano, *An Investigation of the Use of Wavelets in Vibration Applications*, IMAC-XVII, I, 1999, 684–691.

[18] W.J. Staszewski, Identification of Non-Linear Systems using Multi-Scale Ridges and Skeletons of the Wavelet Transform, *Journal of Sound and Vibration* **244**(4) (1998), Article No. SV981616, 639–658.

[19] W.J. Staszewski and J.E. Chance, *Identification of Non-Linear Systems using Wavelets – Experimental Study*, IMAC-XV I, 1997, 1012–1016.